EFFECT OF LOCAL STRESSES ON STATIC STRENGTH AND FATIGUE LIFE OF PATCHED COMPOSITE PANELS

Xiao-Jing Gong, Pengcheng Cheng, Jérôme Rousseau, Shahram Aivazzadeh
Laboratory of Research in Mechanics and Acoustics, Bourgogne University, France

Keywords: *repair; finite element modelling; fatigue*

Abstract

The present study proposes to investigate the effect of local stresses on static tensile strength and fatigue life of some composite structures repaired by bonding composite patches.

The repaired specimens were statically loaded in tension up to failure. The study then focused on the fatigue behaviour of the bonded composite repair system. A series of tests has been realized to observe experimentally different fracture modes. In order to identify the most critical regions in the bonded composite repair system, the field of stresses and deformations has been determined based on finite element approaches.

The effect of local stress concentration on the fatigue life was discussed as a function of patch configurations. It was found that in patched composite repairs the high stress concentration in critical zones leads to early patch debonding and results in low fatigue life.

1 Introduction

The increased use of composite structures in the transport industry (aeronautical and automotive) pose question about the repair of damaged composites structures. In many cases, the cost of complex composite structures is too high to systematically replace damaged ones. A local repair can be considered as a good solution for economical and mechanical reasons.

For the purpose of reconstituting the mechanical performance as close to that of an original structure as possible, one of the repair methods frequently used by industry consists in bonding composite patches to the damaged areas [1]-[6]. Design and realization of this kind of repair have been shown to be very complex. The success of the repair depends on coherence between the base structure material and the patches, the adhesive used, as well as on the skill of repair operators [7].

The aim of this work is to understand how the loads are transmitted from the structure to the repair, where the critical regions are as a function of patch configuration and so to find the key to the optimal design of repair patches. At the beginning, static and cycle tension load was applied to composite system repaired by bonding patches. The distribution of local stresses and deformation were determined by a finite element modelling.

2 Experimental details

2.1 Specimen

The composite structure to repair is a quasi-isotropic laminate in carbon/epoxy with stacking sequence: $[45/-45/0/90]_S$. The repair patches use the same composite with different stacking sequence. The specimens have 250mm long by 50mm wide. A circular hole of 10mm in diameter was drilled at the center of the specimens to simulate the result of clearance of a damaged region, and then composite patches are bonded symmetrically on each side of the specimens. Tabs of the geometry of 50 x 50 x 2.5mm are used (Fig. 1).

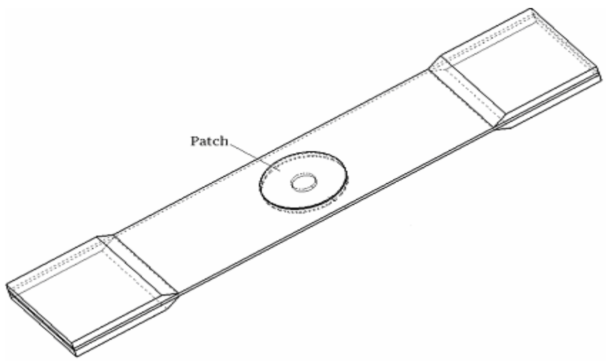

Fig. 1. Specimen

2.2 Patch type

A series of tests have been performed on the specimens repaired by varying different parameters: the nature of patches, their stacking sequence and their geometry; with or without a plug (for filling up the hole), Z-pins (Fig. 2.).

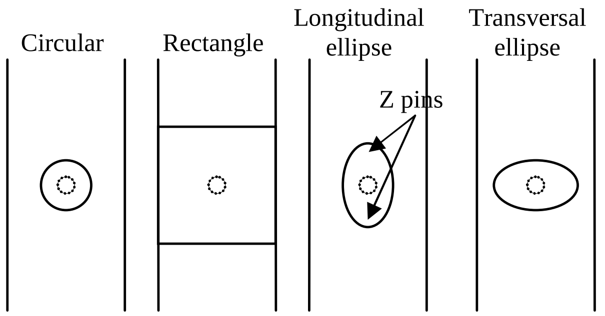

Fig. 2. Geometry of bonded patches

The repair by bonding patches can be realized in two manners:

1) Repair by patches « soft »: the patches non-polymerised are bonded with the composite structure; the patches will be hardened finally. Here an adhesive can be used or not;
2) Repair by patches « hard »: the patches pre-polymerized are bonded directly with the composite structure. Here an adhesive has to be used.

2.3 Static tests

- Repair by «soft» patches of stacking sequence: [45/-45/0/90]

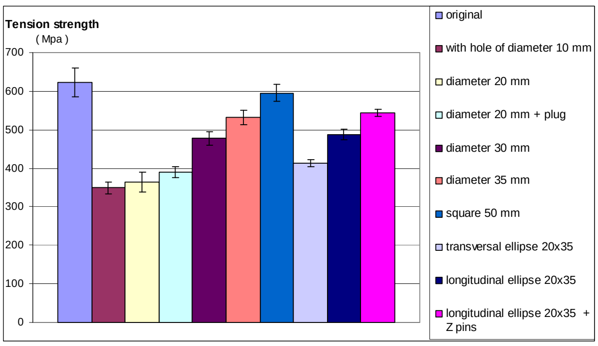

Fig.3. Tension strength of specimens repaired by« soft »patches

The Fig. 3 illustrates the results of static tension tests. The tension strength in term of effective ultimate stress for each patch configuration is compared with that of the undamaged specimen and the specimen with a hole (no repaired). Herein the effective stress is defined as the load of fracture divided by the section surface of the virgin specimen.

It is showed that the square patches, which however, have the biggest adhesive joint surface and so make the system more rigid, do the best repair. The efficacy of circular patches increases with their diameter. For the same bonded surface, the longitudinal ellipse patch appears the most efficient. The application of Z-pins can also improve the repair performance.

The facies of different specimens after fracture are described in Fig. 4.

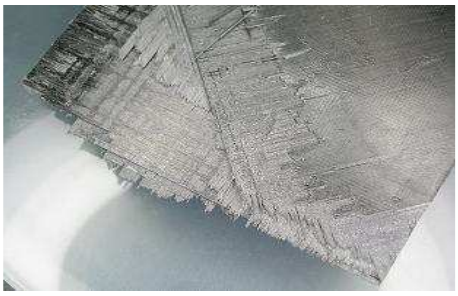

(a) Undamaged specimen

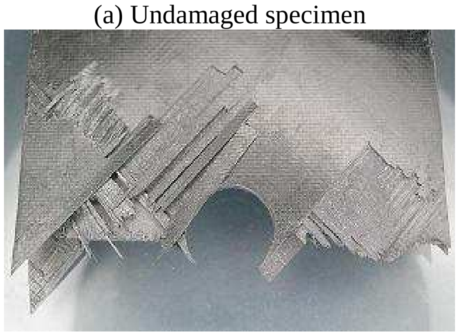

(b) Specimen with a hole

(c) Patched specimen

Fig. 4. Facies of specimen after rupture

- Repair by « hard » patches

For the repairs by «hard» patches, the effect of the material stiffness of applied patches is studied. The patches have 4 layers with the different stacking sequences. Their geometry is always a circle 35 mm in diameter.

The results obtained (Fig. 5) show that the patches $[45/-45]_S$ give a failure strength 25% higher than those $[0/90]_S$. It seems that low stiffness of patches can improve the stress distribution in bonding joint.

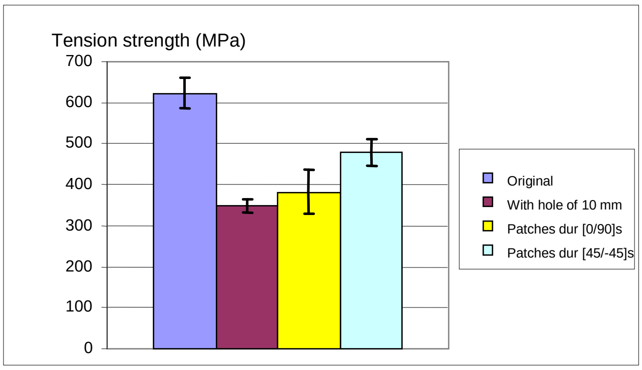

Fig.5. Tension strength of specimens repaired by« hard »patches

2.4 Fatigue test

In order to study the fatigue life in tension of the composite structure repaired by bonding patches, some tests of Traction/Traction (R=0.1) are performed in the present study.

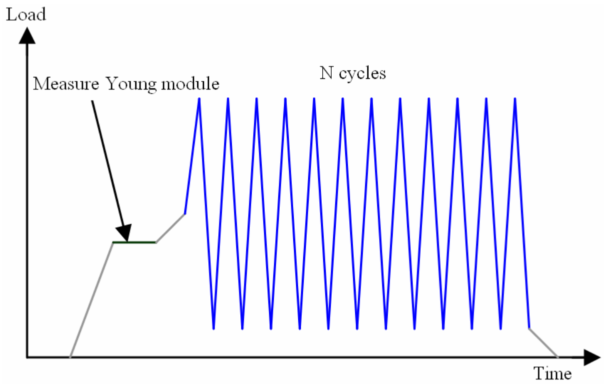

Fig. 6. Fatigue test loading

The Fig. 6 illustrates the typical loading procedure. At beginning the specimen is loaded slowly up to 150MPa, the Young module is measured. And then the cyclic loading (f=3Hz) is applied to the specimen.

- Undamaged specimen

For the undamaged specimens, 2 maximum load levels are chosen: 80% and 60% of ultimate tension strength of static test named σ_0: 498MPa and 374MPa respectively. 5 specimens are tested under 80% σ_0 and 3 others are tested under 60% σ_0. A deadline of 1 million cycles is determined as "infinite life".

The total results are presented in the Fig. 7. The results under loading of 80% of σ_0 are quite dispersed. In the case of 60% of σ_0, only one specimen has been broken at about 1 million cycles, two others resist well up to more than 1 million cycles. The tests were stopped without breaking of the specimens.

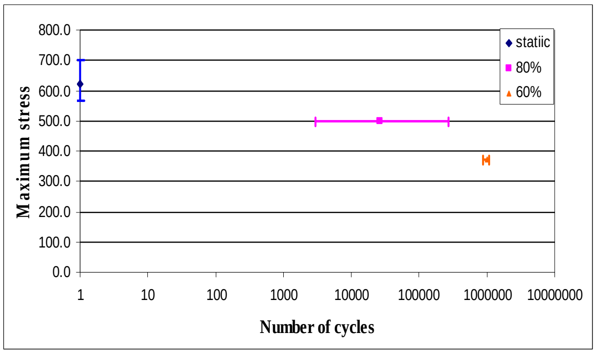

Fig. 7. S-N Results for undamaged specimens

- Patched specimen

After be repaired by « soft » circular patches of 35 mm diameter, 4 specimens are tested under σ_{max}=80% of σ_0; 2 specimens under σ_{max}=60% of σ_0 and σ_{max}=50% of σ_0.

The Fig. 8 illustrates the results. It is seen that the fatigue life under σ_{max}=80% of σ_0 is nearly zero, but that under σ_{max}=60% of σ_0 has the same level than that of undamaged specimens under σ_{max}=80% of σ_0. For the specimens tested under σ_{max}=50% of σ_0, one is broken at 763 000 cycles, another resisted up to more than 2.5 millions cycles.

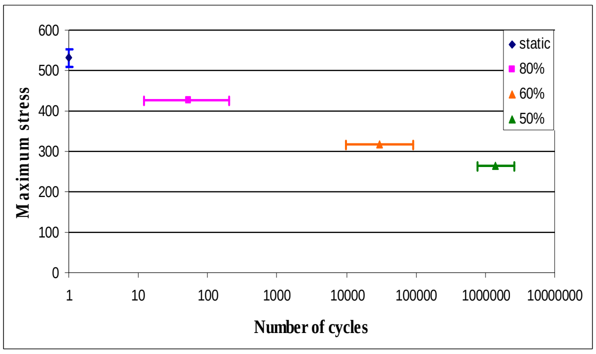

Fig. 8. S-N Results for patched specimens

In order to follow the damage evolution of the repaired composite panels, the control with help of the thermograph method is used during the fatigue tests.

The pictures in Fig. 9 show different steps of damage process. It can be seen that the damage was initiated at the longitudinal edges in the bonding joints of the patches; and then the debonding was growing to the heart of patches; we can see that the patches were detached also at the edges of the hole; finally, the specimens were broken after the detachment of the patches

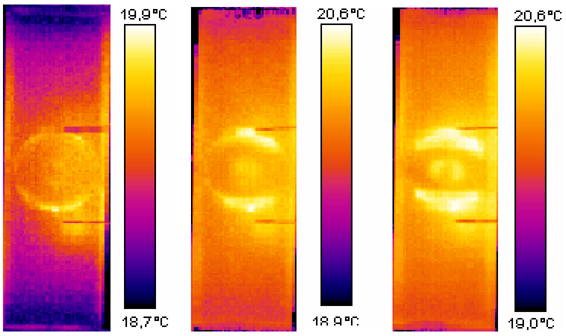

Fig. 9 Different steps on the damage process

3 Finite element analysis

In order to understand the effect of local stresses in the repair patches on their static strength and fatigue life, a finite element analysis is used to determine the distribution of stresses in the repaired specimens.

The software MSC Marc is used in this study. In order to simplify the calculation, the specimen with a hole to repair is considered as three-dimensional orthotropic material. The repair patches are meshed by composite elements ply by ply. The bonding joint is simulated by isotropic adhesive. The calculation is realized in the linear elastic zone.

One extremity of the specimen is fixed. A displacement of 1mm is applied to the other extremity. The Fig. 10 illustrates the meshing model with the definition of 4 critical zones.

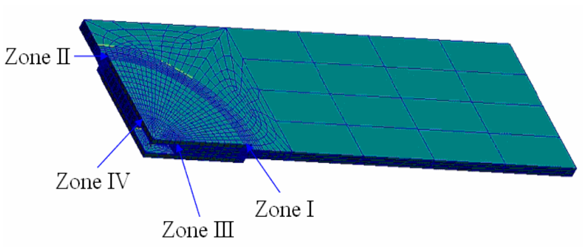

Fig. 10. Meshing model

Two series of patch configurations have been considered.

The patches listed in Table 1 have different stacking sequence. Not only the tensile stiffness of these patches can be varying in a large range, and also the ply angle in contact with the adhesive changes.

The patches listed in Table 2 have the same tensile stiffness, just the ply angle in contact with the adhesive changes.

Table 1. Patches studied in series I

No.	Stacking Sequence*	E_x (GPa)
I-1	$[90]_4$	5.6
I-2	$[45, -45]_s$	25.7
I-3	[90, 0, -45, 45]	35.1
I-4	$[0,90]_s$	44.5
I-5	$[30, -30]_s$	49.9
I-6	$[15, -15]_s$	73.5
I-7	$[0]_4$	83.4

Table 2. Patches studied in series II

No.	Stacking Sequence*
II-A=I-3	[90, 0, -45, 45]
II-B	[-45, 45, 0, 90]
II-C	[0, 90, 45, -45]
II-D	[45, -45, 90, 0]

***** ***The first layer is in contact with the adhesive***

3.1 Localization of critical zones

As mentioned previously, the experimental observation indicates that the damage of patched specimen started at adhesive joint. So, it is important to analyse the stresses distribution in the adhesive interfaces.

The Fig. 11 illustrates the distribution of longitudinal stress σ_x on 4 surfaces in a specimen repaired by the unidirectional 0° patches: S_{1A} designates the surface of patch in contact with the adhesive; S_{2A} the surface of drilled piece in contact with the adhesive; S_{1B} and S_{2B} the surfaces of the adhesive in contact with S_{1A} and S_{2A}. The results indicate that there are 4 zones more loaded: the longitudinal extremity (Zone I) and the transversal extremity (Zone II) of the patches, similarly the longitudinal extremity (Zone III) and the transversal extremity (Zone IV) of the hole.

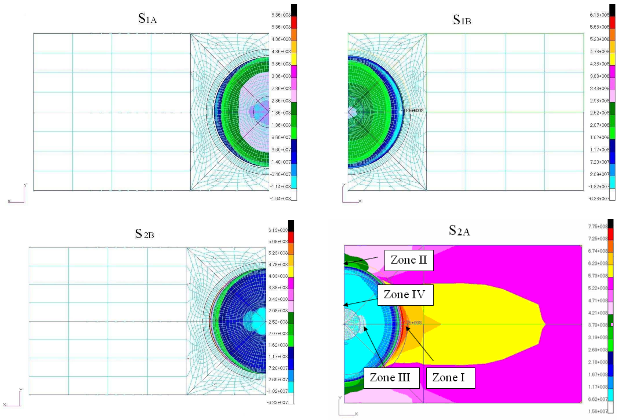

Fig. 11. Distribution of longitudinal stress σ_x

3.2 Maximum effective longitudinal stress in the drilled laminates

In order to comparer the repair efficacy, the longitudinal stress in the drilled laminates is normalized by the average stress in the undamaged specimen, named σ_x*. The results presented in Fig. 12 indicate that the maximal value of σ_x* in the drilled laminates (on the surface S_{1A}) is situated always in the zone I for all patches. The higher the stiffness of the patches is, the more important the value of σ_x*_{max}.

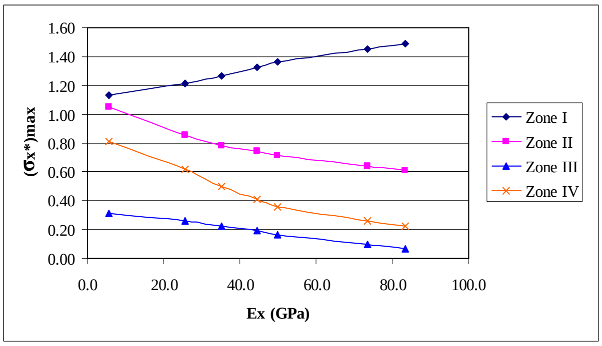

Fig. 12. $(\sigma_x*)_{max}$ vs. E_x for patches in series I

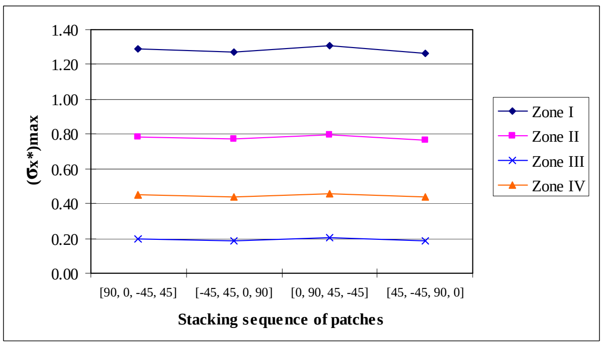

Fig.13 $(\sigma_x*)_{max}$ vs. fibre angle for patches in series II

However, the ply angle in contact with the adhesive seems no influence on this value (Fig. 13).

It is interesting to note that the maximal value of σ_x* in the drilled laminates (non-repair) is equal to 2.8. So, repairs by any patch studied here are more or less helpful to improve the performance of the drilled laminates.

3.3 Stresses in the adhesive

Generally, in a bonded system the adhesive is always the critical element. According to the results obtained by finite element analysis, stresses on the surface S_{2B} are always much higher than those on the surface S_{1B}. So just the results on the surface S_{2B} will be discussed. In Fig. 14 and 15, we can compare the maximal peel stresses in the 4 critical zones for each patch configuration, where the stresses are normalized by the maximum peel stress obtained in the adhesive of repaired specimen with the unidirectional 0° patches.

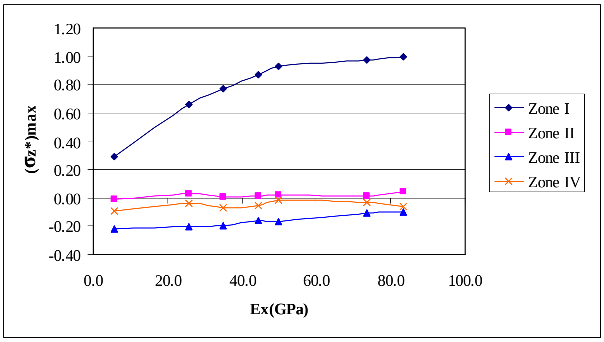

Fig. 14. $(\sigma_z *)_{max}$ vs. E_x for patches in series I

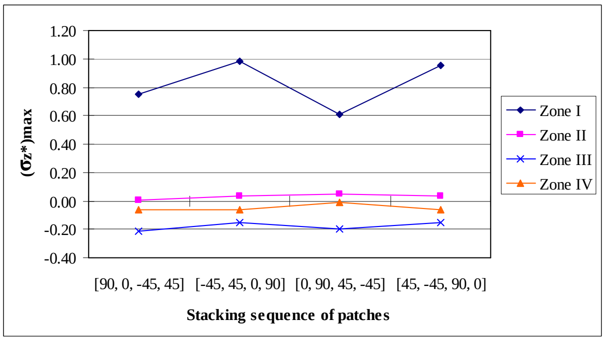

Fig.15 $(\sigma_z*)_{max}$ vs. fibre angle for patches in series II

The zone I is always more critical than the others in all cases. The value of $(\sigma_z*)_{max}$ increases with the module E_x for the patches in the series I.

In the case of the constant module E_x for the patches in the series II, the value of $(\sigma_z^*)_{max}$ varies as a function of the fibre orientation. The fibre angle of 45° or -45° in contact with the adhesive seems to introduce an important pelage stress which is close to the results of the unidirectional 0° patches.

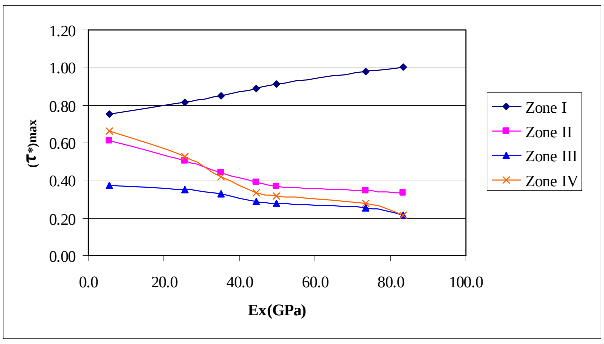

Fig. 16. $(\tau^*)_{max}$ vs. E_x for patches in series I

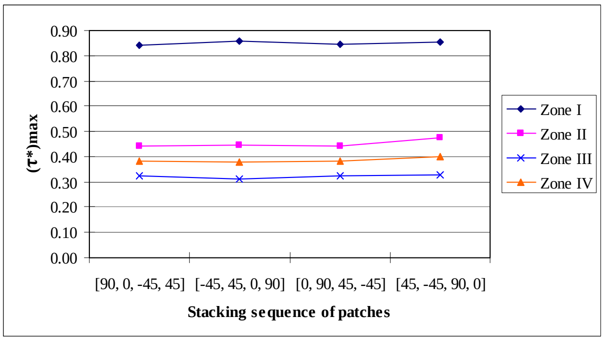

Fig. 17 $(\tau^*)_{max}$ vs. fibre angle for patches in series II

For the shear stress in the adhesive on the surface S_{2B}, the maximal value of (τ^*), witch is normalized by the same method, increases with the module E_x in the zone I, but reduces in the else zones (Fig. 16). In the case of the constant module E_x for the patches in the series II, the variation of the value of $(\tau^*)_{max}$ is not significant (Fig. 17).

3.4 Stresses in the adjacent layer of the patches

Even though the fracture of a patched repaired system under cyclic load is shown by the attachment of the patches, it is not impossible that the damage in the patches could occur firstly, and then develop into the adhesive. In particular, if the adjacent ply of the patches is cracking, the adhesive has to be affected. Therefore, in this part Hoffman's criterion will be applied to analyse this risk on the surface S_{2A}. Eq.1 defines the strength rate R of this criterion:

$$R = \frac{\sigma_1^2 - \sigma_1\sigma_2}{X_t X_c} + \frac{\sigma_2^2}{Y_t Y_c} + \frac{X_c - X_t}{X_t X_c}\sigma_1 + \frac{Y_c - Y_t}{Y_t Y_c}\sigma_2 + \frac{\tau_{12}^2}{S^2} \qquad (1)$$

It is also normalized by the corresponding rate in the case of the unidirectional 0° patches, called R*.

It is indicated that the maximum value of (R*) depends strongly not only on the patch stiffness E_x (Fig. 18), but also on the adjacent fibre orientation and the stacking sequence of patches (Fig. 19).

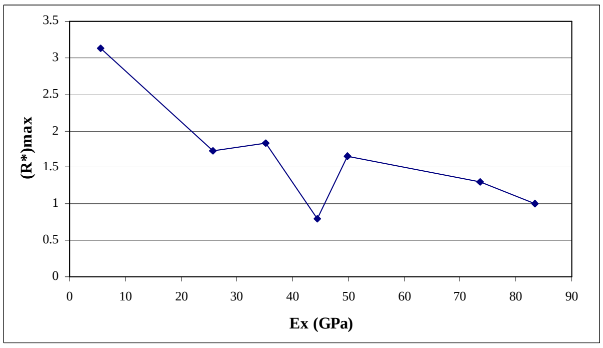

Fig.18. $(R^*)_{max}$ vs. E_x for patches in series I

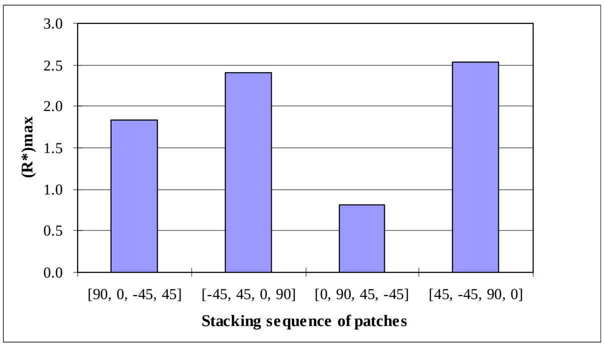

Fig. 19 $(R^*)_{max}$ vs. fibre angle for patches in series II

4 Summary

The results obtained by finite element modelling indicate that the longitudinal extremities of circular patches represent the critical zones where the damage initiates. This conclusion is correlated well with the experimental observation.

The reduction of the tensile stiffness of patches can improve the concentration of the average tensile stress in drilled laminates, the peel stresses and the shear stresses in the adhesive, but favourite the damage of adjacent ply of the patches.

The adjacent ply orientation of the patches influences significantly the shear stress in the adhesive and the strength of the patches. If the tensile stiffness is identical, the 0° adjacent ply angle adhesive gives better distribution.

The presence of the local stress concentration leads to a lower static strength and fatigue life. The key of design optimisation of the repair is to find the best way for load transmission, especially to improve stress concentration in the zone I.

In order to attain this objective, on the one hand, finite element models must take into account of no-linear behaviour of the adhesive, the evolution of damage in the repair; on the other hand, much more static and fatigue tests would be carried out for validation of the calculation by finite element approach.

References

[1] C. Soutis, F. Z. Hu. "Design and performance of bonded patch repairs of composite structure". *Proc Instn Mech Engrs* Vol 211 Part G, 1997.

[2] F. Z. Hu, C. Soutis. "Strength prediction of patch-repaired CFRP laminates loaded in compression". *Composites Science and Technology*, 60, 1103-1114, 2000.

[3] C. Soutis, D. M. Duan, P. Goutas. "Compressive behaviour of CFRP laminates repaired with adhesively bonded external patches". *Composites Structures* 45, 289-301, 1999.

[4] M. N. Charalambides, R. Hardouin, A. J. Kinloch, F. L. Matthews. "Adhesively-bonded repairs to fibre-composite materials I: Experimental". *Composites*, Part A 29A, 1371–1381, 1998.

[5] M. N. Charalambides, A. J. Kinloch, F. L. Matthews. "Adhesively-bonded repairs to fibre-composite materials II: Finite element modelling". *Composites*, Part A 29A, 1383–1396, 1998.

[6] R.D.S.G. Campilho, M.F.S.F. Moura, J.J.M.S. "Modelling single and double-lap repairs on composites materials". *Composites Science and Technology*, 65, 1948-1958, 2005.

[7] J. Rodes, R. Brossier, X.J. Gong, J. Rousseau. "Etude des performances des structures composites réparées". *Matériaux*, Dijon, France, 13-17 Novembre, 2006.